Available online at www.sciencedirect.com
ScienceDirect
Cement and Concrete Research 36 (2006) 2033–2038
Cement and Concrete Research

# Structural and hydration properties of amorphous tricalcium silicate

K. Mori [a,*], T. Fukunaga [a], Y. Shiraishi [a], K. Iwase [b], Q. Xu [a], K. Oishi [c], K. Yatsuyanagi [c], M. Yonemura [d], K. Itoh [a], M. Sugiyama [a], T. Ishigaki [e], T. Kamiyama [d], M. Kawai [d]

[a] Research Reactor Institute, Kyoto University, Kumatori-cho, Sennan-gun, Osaka 590-0494, Japan
[b] Department of Materials Structure Science, Graduate University for Advanced Studies, Tsukuba, Ibaraki 305-0801, Japan
[c] Institute of Technology, Shimizu Corporation, 3-4-17, Etchujima, Koto-ku, Tokyo 135-8530, Japan
[d] Institute of Materials Structure Science, High Energy Accelerator Research Organization, Tsukuba, Ibaraki 305-0801, Japan
[e] Department of Materials Science and Engineering, Muroran Institute for Technology, Muroran 050-8585, Japan

Received 25 April 2005; accepted 16 May 2006

**Abstract**

Mechanical milling was carried out to synthesize amorphous tricalcium silicate ($Ca_3SiO_5$) sample, where $Ca_3SiO_5$ is the most principal component of Portland cement. The partial phase transformation from the crystalline to the amorphous state was observed by X-ray and neutron diffractions. Moreover, it was found that the structural distortion on the Ca–O correlation exists in the milled $Ca_3SiO_5$. The hydration of the milled $Ca_3SiO_5$ with $D_2O$ proceeds as follows: the formation of hydration products such as $Ca(OD)_2$ rapidly occurs in the early hydration stage, and then proceeds slowly after about 15 h. The induction time for the hydration of the milled $Ca_3SiO_5$ is approximately one half shorter than that for the hydration of the unmilled one. This result means that the mechanical milling brings about the chemical activity of $Ca_3SiO_5$ for hydration, and may be particularly useful for increasing the reactivity in the early hydration stage.


*Keywords:* $Ca_3SiO_5$; Amorphous material; Crystal structure; Hydration; Neutron scattering

## 1. Introduction

Portland cement clinkers have been recognized to be very important materials for constructing various kinds of concrete buildings. The concrete properties such as compressive strength, durability and hydration are strongly associated with the water-to-cement ratio and the size distribution of the cement particle [1,2]. For further improvement in cement (or concrete) properties, many extensive studies have been carried out from various viewpoints [3–7]. In the meantime, mechanical milling has been paid much attention for synthesizing amorphous or metastable alloys. This process is also well known to promote the reactivity of various materials: biomaterials and energy stored materials [8–12]. Therefore, it can be easily expected that the application of the mechanical milling to the hydration process of cement will improve the concrete properties. Although the importance of the particle size of the cement clinker has been discussed frequently [1], the effect of amorphization may be insufficiently understood. In the hydration process of cement, the creation of cement hydration products may strongly depend on the solubility of Ca ions in water. Therefore, we should focus on the instability of Ca ions in the amorphization cement. Especially, the detailed structural information of the milled cement in atomic level is indispensable to elucidate its hydration process.

In the present research, we studied the hydration process from the structural viewpoint by taking advantage of time-of-flight neutron powder diffraction (TOF-NPD) by focusing on $Ca_3SiO_5$ of the major component of Portland cement clinkers, and by using mechanical milling technique for the improvement of concrete properties. The TOF-NPD is an excellent method for elucidating positions of not only constituent elements but also hydrogen (deuterium) after hydration in Portland cement. Moreover, the local atomic configuration for the milled $Ca_3SiO_5$ was investigated by pair distribution function method.

* Corresponding author. Tel.: +81 724 51 2363; fax: +81 724 51 2635.
*E-mail address:* kmori@rri.kyoto-u.ac.jp (K. Mori).

0008-8846/$ - see front matter © 2006 Elsevier Ltd. All rights reserved.
doi:10.1016/j.cemconres.2006.05.004

## 2. Experimental

Polycrystalline $Ca_3SiO_5$ was synthesized by conventional ceramic processing from $CaCO_3$ (99.99%) and $SiO_2$ (99.9%) powders, which were well mixed in the molar proportion. The mixture was heated at 900 °C for 12 h in air. After grinding, the sample was pressed into disks and heated at 1500 °C for 12 h in air to make it more uniform. In order to refine the crystal structure of $Ca_3SiO_5$, the TOF-NPD was carried out using the versatile neutron powder diffractometer, Vega, installed at the pulsed neutron source of Neutron Science Laboratory (KENS) in High Energy Accelerator Research Organization (KEK) [13]. The resolution of Vega, defined as $\Delta d/d$, is approximately 0.2%. The sample was put into a cylindrical vanadium cell that has a diameter of 9.2 mm, a height of 65 mm and a thickness of 0.2 mm. The Rietveld method was employed the obtained TOF-NPD data of $Ca_3SiO_5$ [14,15]. The mechanical milling was conducted dry at 200 rpm for 30 h under argon gas atmosphere using a planetary ball mill apparatus (Fritsch Pulverisette 5). Steel balls with a diameter of 10 mm and a steel pot were utilized as milling media. The X-ray powder diffraction (XPD) patterns of the milled $Ca_3SiO_5$ were measured with the X-ray diffractometer (RAD-C, Rigaku Corporation) with Cu-$K_\alpha$ radiation (40 kV, 30 mA). No Bragg peaks of steel appear on the X-ray diffraction pattern. The particle size distribution (PSD) for each sample was measured using laser diffraction technique (MT3300EX II, Nikkiso Corporation), and the photographs of the unmilled and milled $Ca_3SiO_5$ were taken by the scanning electron microscopy (SEM). The local structures of both samples were investigated using the high intensity total scattering spectrometer, HIT-II, at KEK-KENS. The sample was put into a cylindrical Ti–Zr null-alloy cell that is 8.0 mm in inner diameter and 0.3 mm in thickness. The radial distribution functions, RDF($r$), were derived from the Fourier transformation of the structure factors, $S(Q)$, by truncating at $Q$=45 Å$^{-1}$. In hydration process of the milled $Ca_3SiO_5$, heavy water ($D_2O$) was used to suppress the incoherent scattering of H atoms. Note that reaction of $Ca_3SiO_5$ with $D_2O$ is significantly reacted in comparison to reaction $H_2O$ [16]. However, this does

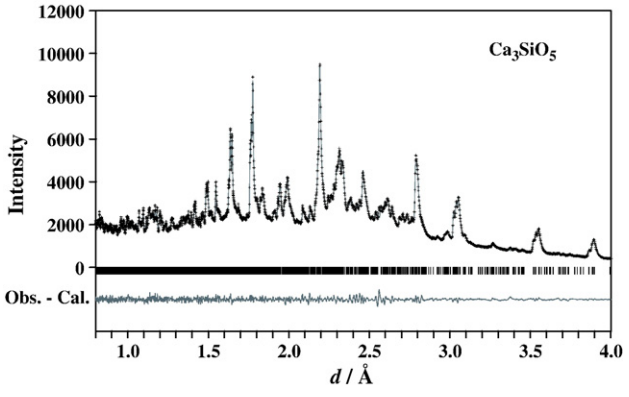


Fig. 1. Full pattern of Rietveld analysis result for the $Ca_3SiO_5$. The plus marks are the observed neutron diffraction intensities, and the solid line is the caluculated ones. The vertical marks below the profile indicate the positions of the Bragg reflections. The curve at the bottom is the difference between the observed and the calculated intensities.

Table 1
Refined structure parameters of $Ca_3SiO_5$ at RT

| Atom | x | y | z |
|---|---|---|---|
| Ca(1) | 0.716(3) | −0.010(2) | 0.962(2) |
| Ca(2) | 0.376(2) | 0.074(2) | 0.687(1) |
| Ca(3) | 0.648(2) | 0.312(2) | 0.330(2) |
| Ca(4) | 0.846(2) | 0.172(2) | 0.177(2) |
| Ca(5) | 0.189(2) | 0.343(2) | 0.823(2) |
| Ca(6) | 0.328(2) | 0.418(2) | 0.667(2) |
| Ca(7) | 0.666(2) | 0.088(2) | 0.334(2) |
| Ca(8) | 0.043(2) | 0.175(2) | 0.626(2) |
| Ca(9) | 0.624(2) | 0.161(2) | 0.704(2) |
| Ca(10) | 0.390(2) | 0.319(2) | 0.303(2) |
| Ca(11) | 0.963(2) | 0.333(2) | 0.361(2) |
| Ca(12) | 0.039(2) | 0.418(2) | 0.623(2) |
| Ca(13) | 0.382(2) | 0.059(2) | 0.306(2) |
| Ca(14) | 0.619(2) | 0.444(2) | 0.694(2) |
| Ca(15) | 0.956(2) | 0.102(2) | 0.368(2) |
| Ca(16) | 0.476(2) | 0.081(2) | 0.856(2) |
| Ca(17) | 0.231(2) | 0.250(2) | 0.461(2) |
| Ca(18) | 0.811(2) | 0.268(2) | 0.546(2) |
| Ca(19) | 0.520(2) | 0.404(2) | 0.151(2) |
| Ca(20) | 0.664(2) | 0.466(2) | 0.908(2) |
| Ca(21) | 0.717(2) | 0.224(2) | 0.959(2) |
| Ca(22) | 0.321(2) | 0.290(2) | 0.044(2) |
| Ca(23) | 0.865(2) | 0.094(2) | 0.801(2) |
| Ca(24) | 0.162(2) | 0.406(2) | 0.167(2) |
| Ca(25) | 0.012(2) | 0.263(2) | 1.002(2) |
| Ca(26) | 0 | 0 | 0 |
| Ca(27) | 0 | 1/2 | 0 |
| Ca(28) | 1/2 | 0 | 1/2 |
| Ca(29) | 1/2 | 1/2 | 1/2 |
| Si(1) | 0.861(2) | 0.413(3) | 0.178(2) |
| Si(2) | 0.455(2) | 0.352(2) | 0.880(2) |
| Si(3) | 0.161(3) | 0.083(3) | 0.833(3) |
| Si(4) | 0.796(3) | 0.017(2) | 0.543(2) |
| Si(5) | 0.194(3) | 0.496(2) | 0.446(2) |
| Si(6) | 0.465(2) | 0.221(2) | 0.140(2) |
| Si(7) | 0.130(3) | 0.172(3) | 0.202(2) |
| Si(8) | 0.857(2) | 0.320(3) | 0.796(2) |
| Si(9) | 0.504(3) | 0.235(2) | 0.496(2) |
| O(1) | 0.031(2) | 0.178(2) | 0.273(2) |
| O(2) | 0.534(2) | 0.268(2) | 0.189(2) |
| O(3) | 0.635(2) | 0.146(2) | 0.085(2) |
| O(4) | 0.138(2) | 0.065(2) | 0.151(2) |
| O(5) | 0.189(2) | 0.324(2) | 0.665(2) |
| O(6) | 0.499(2) | 0.030(2) | 0.678(2) |
| O(7) | 0.427(2) | 0.126(2) | 0.038(2) |
| O(8) | 0.264(2) | 0.186(2) | 0.291(2) |
| O(9) | 0.651(2) | 0.088(2) | 0.839(2) |
| O(10) | 0.009(2) | 0.257(2) | 0.480(2) |
| O(11) | 0.512(2) | 0.071(2) | 0.195(2) |
| O(12) | 0.161(2) | 0.267(2) | 0.167(2) |
| O(13) | 0.826(2) | 0.396(2) | 0.463(2) |
| O(14) | 0.303(2) | 0.465(2) | 0.411(2) |
| O(15) | 0.181(2) | 0.411(2) | 0.523(2) |
| O(16) | 0.354(2) | 0.429(2) | 0.189(1) |
| O(17) | 0.134(2) | 0.373(2) | 0.997(2) |
| O(18) | 0.087(2) | 0.446(2) | 0.343(1) |
| O(19) | 0.286(2) | 0.025(2) | 0.781(2) |
| O(20) | 0.949(2) | 0.396(2) | 0.114(2) |
| O(21) | 0.170(2) | 0.194(2) | 0.879(2) |
| O(22) | 0.139(2) | 0.016(2) | 0.896(2) |
| O(23) | 0.835(2) | 0.200(2) | 0.335(1) |
| O(24) | 0.890(2) | 0.120(2) | 1.011(2) |
| O(25) | 0.570(2) | 0.461(2) | 0.324(1) |
| O(26) | 0.064(2) | 0.065(2) | 0.751(2) |

Table 1 (*continued*)

| Atom | *x* | y | z |
|---|---|---|---|
| O(27) | 0.617(2) | 0.250(2) | 0.437(2) |
| O(28) | 0.772(2) | 0.037(2) | 0.669(2) |
| O(29) | 0.456(2) | 0.372(2) | 0.971(2) |
| O(30) | 0.594(2) | 0.306(2) | 0.853(2) |
| O(31) | 1.016(2) | 0.301(2) | 0.741(1) |
| O(32) | 0.678(2) | 0.008(2) | 0.481(2) |
| O(33) | 0.856(2) | 0.240(2) | 0.847(2) |
| O(34) | 0.704(2) | 0.399(2) | 0.073(2) |
| O(35) | 0.744(2) | 0.297(2) | 0.690(2) |
| O(36) | 0.874(2) | 0.096(2) | 0.511(2) |
| O(37) | 0.845(2) | 0.410(1) | 0.855(2) |
| O(38) | 0.425(2) | 0.138(2) | 0.467(2) |
| O(39) | 0.117(2) | 0.076(2) | 0.438(2) |
| O(40) | 0.776(2) | 0.324(2) | 0.232(2) |
| O(41) | 0.433(2) | 0.212(2) | 0.801(2) |
| O(42) | 0.520(2) | 0.290(2) | 0.627(2) |
| O(43) | 0.398(2) | 0.333(1) | 0.490(2) |
| O(44) | 0.168(2) | 0.464(2) | 0.762(2) |
| O(45) | 0.464(2) | 0.417(2) | 0.806(2) |

not affect the direct comparison of milled and unmilled powder in our experiments. The $D_2O$-to-$Ca_3SiO_5$ mass ratio is fixed to be 0.5. After mixing the milled $Ca_3SiO_5$ with $D_2O$ under argon gas, the mixture was sealed into a cylindrical vanadium cell. Then, the NPD experiments using the Vega spectrometer were performed over about 6 days.

## 3. Results

### 3.1. Crystal structure of $Ca_3SiO_5$

Fig. 1 shows a final profile fit to the TOF-NPD data of $Ca_3SiO_5$ at room temperature (RT). The structure parameters of $Ca_3SiO_5$ including 83 atomic sites were refined on the basis of the triclinic phase (space group: $P\bar{1}$) [17,18]. In the Rietveld refinement, the occupancies at all atomic sites were fixed at unity. As shown in Fig. 1, a good coincidence was obtained between the observed and calculated patterns ($R_{wp}$=3.33% and $S$=2.6419, where $R_{wp}$ and $S$ are the $R$-factor and the goodness-of-fit, respectively). In addition, this result is in good agreement with that reported in our previous work [19]. Therefore, we could confirm that the excellent polycrystalline sample of $Ca_3SiO_5$ was prepared. From the result of the Rietveld analysis, lattice parameters of $Ca_3SiO_5$ were estimated as follows: $a$=11.6311(3) Å, $b$=14.2102(4) Å, $c$=13.6832(4) Å, $\alpha$=105.297(2)°, $\beta$=94.560(2)° and $\gamma$=89.838 (3)°. The structure parameters of $Ca_3SiO_5$ are summarized in Table 1. A schematic illustration of $Ca_3SiO_5$ is shown in Fig. 2. It is most likely that [$SiO_4$] tetrahedra are isolated in this system.

### 3.2. Local structure of the milled $Ca_3SiO_5$

Fig. 3 shows a series of XPD patterns of $Ca_3SiO_5$ for 0 h (unmilled), 10 h, 20 h and 30 h of milling. All Bragg reflections became gradually broader when the mechanical milling proceeds, even though the Bragg peaks do not move in position. Fig. 4a and b show SEM photographs of the unmilled $Ca_3SiO_5$ and milled one after 30 h of milling, respectively. It is clearly recognized that

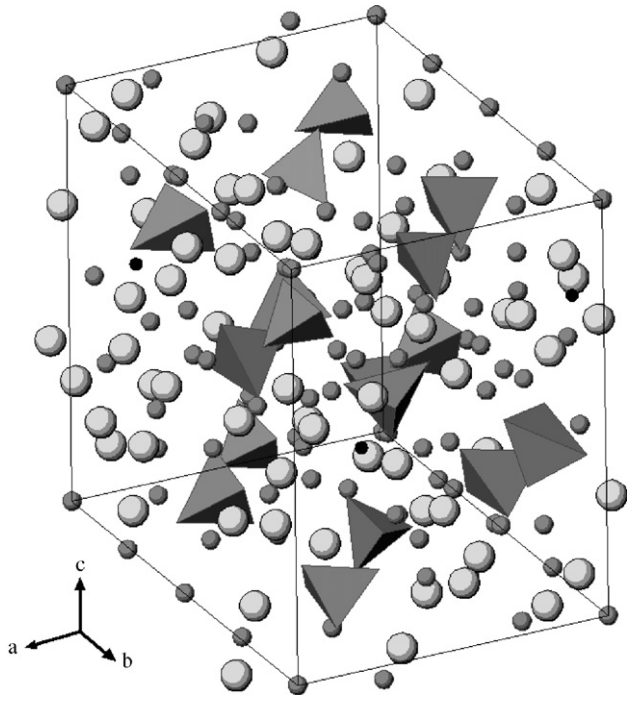


Fig. 2. Schematic illustration of $Ca_3SiO_5$ at RT obtained from the result of the Rietveld analysis. The [$SiO_4$] tetrahedra are indicated in dark grey. The spheres of grey, black and white correspond to Ca, Si and O atoms, respectively.

the unmilled $Ca_3SiO_5$ mainly consists of tabular particles, while the spherical ones can be observed in the milled $Ca_3SiO_5$. The PSD of each sample is demonstrated in Fig. 5. Although the number of particles with small size (<20 μm) slightly increases in the milled $Ca_3SiO_5$, it is most likely that the average sizes of both samples are almost the same. Thus, the PSD was recognized to scarcely change from the result of PSD measurements, however the peak profile of X-ray pattern for the milled $Ca_3SiO_5$ became obviously broad in comparison with that for the unmilled one. These results may allow us to understand that the mechanical milling resulted in partial amorphization of $Ca_3SiO_5$.

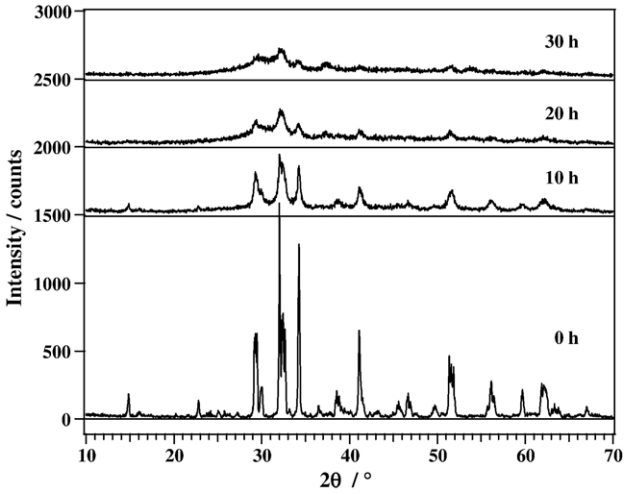


Fig. 3. X-ray diffraction patterns of $Ca_3SiO_5$ after 0 h (unmilled), 10 h, 20 h and 30 h of milling.

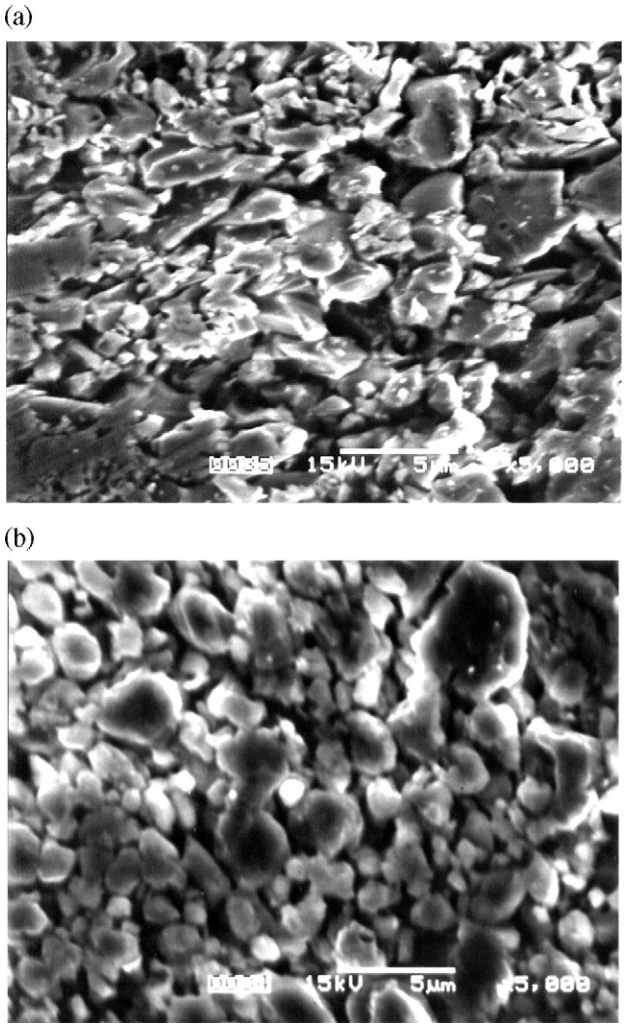


Fig. 4. SEM photographs of the unmilled (a) and milled $Ca_3SiO_5$ (b).

In order to get more insight of the atomic structure of the unmilled and milled $Ca_3SiO_5$, $S(Q)$'s were measured by the HIT-II, and then the RDF($r$)'s of both samples were derived from the Fourier transformation of $S(Q)$'s. Fig. 6 shows the

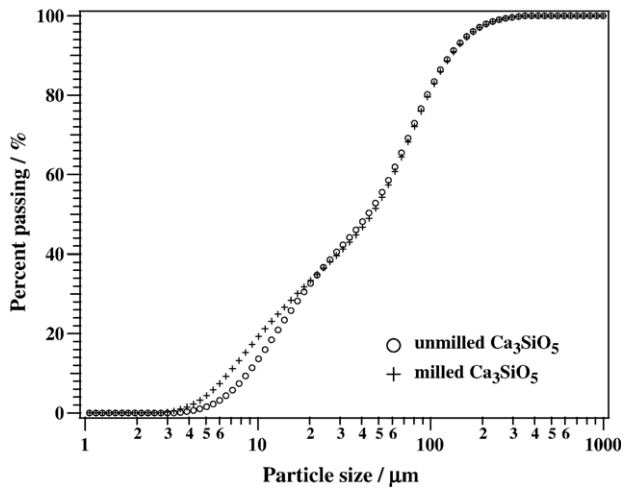


Fig. 5. Measured particle size distributions for the unmilled and milled $Ca_3SiO_5$.

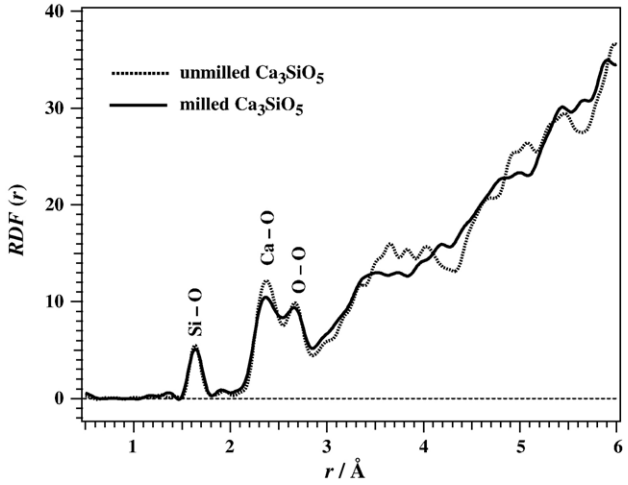


Fig. 6. Radial distribution functions, RDF($r$), of the unmilled and milled $Ca_3SiO_5$, respectively. The RDF($r$) is defined as follows:

$$\mathrm{RDF}(r) = 4\pi r^2\rho + \frac{2r}{\pi}\int_0^\infty Q\{S(Q)-1\}\sin(Qr)\mathrm{d}Q,$$

where $\rho$ is the average number density of atoms, which was estimated from the result of Rietveld refinement of $Ca_3SiO_5$.

comparison between the RDF($r$)'s of the unmilled and milled $Ca_3SiO_5$. In the RDF($r$), the first peak at around 1.6 Å indicates the Si–O correlation in a [$SiO_4$] tetrahedron, because the coordination number of Si–O was calculated to be 4 oxygen atoms around a Si atom from the area of the first peak. Furthermore, the correlation length of the Si–O is almost the same as those in $SiO_2$ and $CaSiO_3$ glasses [20]. The second and third peaks can be recognized to correspond to the Ca–O correlation (~2.4 Å) and the O–O one (~2.7 Å), respectively. As shown in Fig. 6, the peak profiles of Si–O and O–O correlations of the milled $Ca_3SiO_5$ do not change in comparison with those of the unmilled $Ca_3SiO_5$, whereas the peak broadening of Ca–O correlation is conspicuous. This result leads us

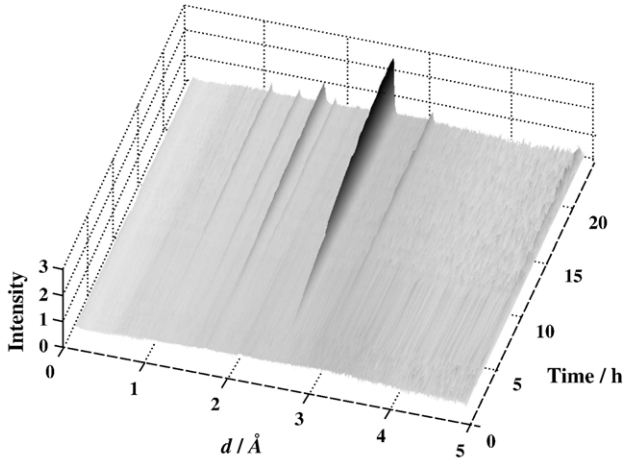


Fig. 7. Change of the neutron powder diffraction pattern of the hydrated milled $Ca_3SiO_5$ up to 24 h of hydration.

to understand that the structural distortion took place around Ca atoms due to various kinds of defects was induced by mechanical milling.

### 3.3. Hydration properties of the milled $Ca_3SiO_5$

Fig. 7 displays a surface-plot of the change in the TOF-NPD pattern during the hydration process of the milled $Ca_3SiO_5$ with $D_2O$ up to 24 h of hydration. Several Bragg reflections are drastically growing in these TOF-NPD patterns. Fig. 8 shows the final Rietveld refinement pattern of the milled $Ca_3SiO_5$ hydrated for about 6 days. In this Rietveld analysis, two components of the calcium hydroxide ($Ca(OD)_2$) and unhydrated $Ca_3SiO_5$ were assumed to exist in this specimen, since the hydration formula is generally written as follows: $Ca_3SiO_5+(3+y-x)H_2O\rightarrow(CaO)_x(SiO_2)(H_2O)_y+(3-x)Ca(OH)_2$ [21,22], where $(CaO)_x(SiO_2)(H_2O)_y$ is the calcium silicate hydrate (C–S–H, amorphous state) such as tobermorite and jennite [23–25]. All structure parameters of the milled $Ca_3SiO_5$ except the scale factor and profile function parameters were fixed at the same values obtained from the Rietveld analysis of $Ca_3SiO_5$. Furthermore, we applied a trigonal phase (space group: $P\bar{3}m1$) to the crystal structure model of $Ca(OD)_2$. The fairly good fit was obtained between the observed and calculated patterns ($R_{wp}$=2.74%, $S$=1.4141), as shown in Fig. 8. The lattice parameters of $Ca(OD)_2$ are $a$=3.5934(1) Å and $c$=4.9046(3) Å, respectively. The atomic coordinates of $Ca(OD)_2$ are estimated as follows: Ca(0, 0, 0), D(1/3, 2/3, 0.576 (1)) and O(1/3, 2/3, 0.767(1)). This result is in good agreement with the previous reports on the structure of the hydrated $Ca_3SiO_5$ and the single-crystal of $Ca(OD)_2$ [19,26].

To evaluate the improvement of the early hydration properties (<24 h of hydration) subjected by mechanical milling, the intensities for the 101 reflection ($d\sim$2.63 Å) of $Ca(OD)_2$ were estimated for all TOF-NPD data of the unmilled and milled $Ca_3SiO_5$. Fig. 9 shows the time dependence of intensities for the 101 reflection of $Ca(OD)_2$ for each sample. In the case of the hydrated unmilled $Ca_3SiO_5$, the diffraction data

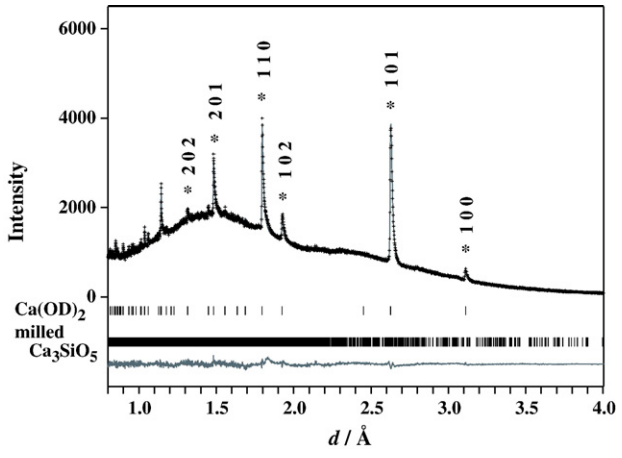


Fig. 8. Rietveld refinement pattern of the hydrated milled $Ca_3SiO_5$ after about 6 h of hydration. The calculated pattern includes two phases: milled $Ca_3SiO_5$ and $Ca(OD)_2$. The Bragg reflections of $Ca(OD)_2$ are indicated as "∗".

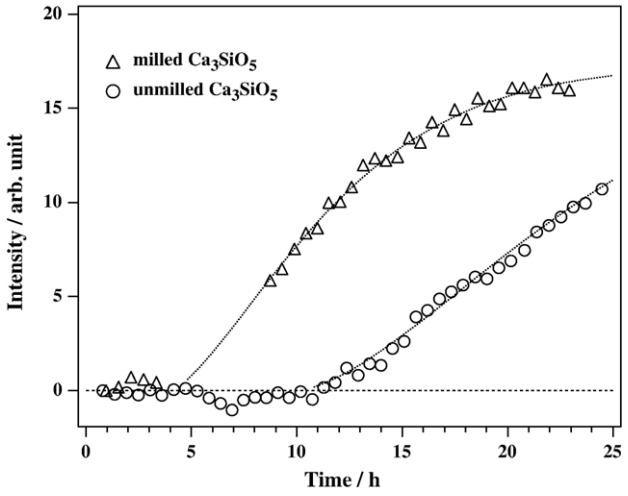


Fig. 9. Time dependence of intensities for the 101 reflection of $Ca(OD)_2$ for the hydrated unmilled and hydrated milled $Ca_3SiO_5$. The broken lines are the guide to the eyes.

in the early hydration stage show no sign of the $Ca(OD)_2$ phase, while the Bragg reflection of $Ca(OD)_2$ gradually appears after 10 h of hydration. On the other hand, the creation of $Ca(OD)_2$ in the hydrated milled $Ca_3SiO_5$ is remarkably accelerated even for 10 h of hydration. In particular, the induction time of the hydrated milled $Ca_3SiO_5$ is approximately one half shorter than that of the hydrated unmilled one. After about 15 h of hydration, it seems that the hydration rate of the milled $Ca_3SiO_5$ is suppressed slowly.

## 4. Discussion

In the evaluation of the hydration properties of $Ca_3SiO_5$, we could demonstrate that mechanical milling enhanced the chemical activity in the early hydration stage. Especially, the induction time in the hydrated milled $Ca_3SiO_5$ was approximately one half shorter than that in the hydrated unmilled one, as shown in Fig. 9. The improvement of the reactivity by mechanical milling may be concerned with the amorphization of $Ca_3SiO_5$ rather than the decrease in the particle size of $Ca_3SiO_5$. Because, the PSD experiments showed that mechanical alloying scarcely affects the reduction in the particle size of $Ca_3SiO_5$, whereas the XPD experiments of $Ca_3SiO_5$ indicated that this process brings about partially the phase transformation from the crystalline to the amorphous state. In the local structure analyses of the unmilled and milled $Ca_3SiO_5$, it was found that ball milling results in the formation of various kinds of defects around Ca atoms when the amorphization of $Ca_3SiO_5$ proceeds. This means that the bonding of the Ca–O correlation is extremely weaker than that of the Si–O correlation. As mentioned in Introduction, the hydration rate of cement paste strongly depends on the solubility of $Ca^{2+}$ ions in free water. Since the activated $Ca^{2+}$ ions induced by mechanical milling may rapidly dissolve in free water, it can be recognized that the hydration may be accelerated in the early stage. Therefore, it is worth noting that mechanical milling is particularly useful for increasing the reactivity in the early hydration stage.

## 5. Conclusion

Polycrystalline $Ca_3SiO_5$ could be synthesized as a single-phase material. The crystal structure was refined as the triclinic phase using the TOF-NPD and the Rietveld methods. For the same sample, high-energy ball milling was employed to enhance the activity of $Ca_3SiO_5$. From the results of the SEM, PSD and XPD experiments, it was found that mechanical milling induces the partial phase transformation from the crystalline to the amorphous state. Especially, it was revealed that the amorphization of $Ca_3SiO_5$ arises from the local deformation of the atomic arrangement around a Ca atom through the short-range structure observed by pair distribution function method. The mechanically activated $Ca_3SiO_5$ became rapidly hydrated in the early hydration stage, and then the formation of hydration products (e.g. $Ca(OD)_2$) was gradually suppressed after about 15 h of hydration. The higher reaction of the milled $Ca_3SiO_5$ may strongly depend on the structure defects introduced by mechanical milling.

## Acknowledgement

We wish to acknowledge Professor T. Yoshiie of Research Reactor Institute of Kyoto University (KURRI) for valuable technical support of SEM experiments. Many thanks are given to the NPD group of KENS at KEK. This work was supported by a Grant-in-Aid for Creative Scientific Research from the Ministry of Education, Science, Sports and Culture, Japan.

## References

[1] D.P. Bentz, C.J. Haecker, An argument for using coarse cements in high-performance concretes, Cem. Concr. Res. 29 (1999) 615–618.
[2] R. Berliner, M. Popovici, K.W. Herwig, M. Berliner, H.M. Jennings, J.J. Thomas, Quasielastic neutron scattering study of the effect of water-to-cement ration on the hydration kinetics of tricalcium silicate, Cem. Concr. Res. 28 (1998) 231–243.
[3] H.W.F. Taylor, Cement Chemistry, second ed., Thomas Telford, London, 1997.
[4] K. Fujii, W. Kondo, Kinetics of the hydration of tricalcium silicate, J. Am. Ceram. Soc. 57 (11) (1974) 492–497.
[5] M. Tarrida, M. Madon, B.L. Rolland, P. Colombet, An in-situ Raman spectroscopy study of the hydration of tricalcium silicate, Adv. Cem. Base7d Mater. 2 (1995) 15–20.
[6] S.A. FitzGerald, D.A. Neumann, J.J. Rush, D.P. Bentz, R.A. Livingston, In situ quasi-elastic neutron scattering study of the hydration of tricalcium silicate, Chem. Mater. 10 (1998) 397–402.
[7] R.A. Livingston, Fractal nucleation and growth model for the hydration of tricalcium silicate, Cem. Concr. Res. 30 (2000) 1853–1860.
[8] U. Gbureck, O. Grolms, J.E. Barralet, L.M. Grover, R. Thull, Mechanical activation and cement formation of β-tricalcium phosphate, Biomaterials 24 (2003) 4123–4131.
[9] U. Gbureck, J.E. Barralet, L. Radu, H.G. Klinger, R. Thull, Amorphous α-tricalcium phosphate: preparation and aqueous setting reaction, J. Am. Ceram. Soc. 87 (6) (2004) 1126–1132.
[10] C.L. Camiré, U. Gbureck, W. Hirsiger, M. Bohner, Correlating crystallinity and reactivity in an α-tricalcium phosphate, Biomaterials 26 (2005) 2787–2794.
[11] T. Fukunaga, K. Nagano, U. Mizutani, H. Wakayama, Y. Fukushima, Structural change of graphite subjected to mechanical milling, J. Non-Cryst. Solids 232–234 (1998) 416–420.
[12] S. Orimo, G. Majer, T. Fukunaga, A. Züttel, L. Schlapbach, H. Fujii, Hydrogen in the mechanically prepared natostructured graphite, Appl. Phys. Lett. 75 (1999) 3093–3095.
[13] T. Kamiyama, K. Oikawa, N. Tsuchiya, M. Osawa, H. Asano, N. Watanabe, M. Furusaka, S. Satoh, I. Fujikawa, T. Ishigaki, F. Izumi, A new TOF neutron powder diffractometer with arrays of one-dimensional PSD's, Physica B 213–214 (1995) 875–877.
[14] H.M. Rietveld, A profile refinement method for nuclear and magnetic structures, J. Appl. Crystallogr. 2 (1969) 65–71.
[15] T. Ohta, F. Izumi, K. Oikawa, T. Kamiyama, Rietveld analysis of intensity data taken on the TOF neutron powder diffractometer VEGA, Physica B 234–236 (1997) 1093–1095.
[16] J.J. Thomas, H.M. Jennings, Effect of D2O and mixing on the early hydration kinetics of tricalcium silicate, Chem. Mater. 11 (1999) 1907–1914.
[17] N.I. Golovastikov, R.G. Matveeva, N.V. Belov, Crystal structure of the tricalcium silicate $3CaO{\cdot}SiO_2 = C_3S$, Sov. Phys. Crystallogr. 20 (4) (1975) 441–445.
[18] R. Berliner, C. Ball, P.B. West, Neutron powder diffraction investigation of model cement compounds, Cem. Concr. Res. 27 (4) (1997) 551–575.
[19] K. Mori, K. Yatsuyanagi, K. Oish, T. Fukunaga, T. Kamiyama, T. Ishigaki, A. Hoshikawa, S. Harjo, K. Iwase, K. Itoh, M. Kawai, Structural studies of hydrated tricalcium silicate by neutron powder diffraction, J. Neural Res. 13 (1–3) (2005) 163–167.
[20] C.D. Yin, M. Okuno, H. Morikawa, F. Marumo, T. Yamanaka, Structural analysis of $CaSiO_3$ glass by X-ray diffraction and Raman spectroscopy, J. Non-Cryst. Solids 80 (1986) 167–174.
[21] S.A. FitzGerald, J.J. Thomas, D.A. Neumann, R.A. Livingston, A neutron scattering study of the role of diffraction in the hydration of tricalcium silicate, Cem. Concr. Res. 32 (2002) 409–413.
[22] S.A. FitzGerald, D.A. Neumann, J.J. Rush, D.P. Bentz, R.A. Livingston, In situ quasi-elastic neutron scattering study of the hydration of tricalcium silicate, Chem. Mater. 10 (1998) 397–402.
[23] J.J. Chen, J.J. Thomas, H.F.W. Taylor, H.M. Jennings, Solubility and structure of calcium silicate hydrate, Cem. Concr. Res. 34 (2004) 1499–1519.
[24] E. Bonaccorsi, S. Merlino, H.F.W. Taylor, The crystal structure of jennite, $Ca_9Si_6O_{18}(OH)_6{\cdot}8H_2O$, Cem. Concr. Res. 34 (2004) 1481–1488.
[25] A. Nonat, The structure and stoichiometry of C–S–H, Cem. Concr. Res. 34 (2004) 1521–1528.
[26] L. Desgranges, D. Grebille, G. Calvarin, Hydrogen thermal motion in calcium hydroxide: $Ca(OH)_2$,, Acta Crystallogr., B 49 (1993) 812–817.